ELSEVIER

PII: S0032-3861(97)00080-3

Polymer Vol. 38 No. 21, pp. 5339–5345, 1997

0032-3861/97/$17.00+0.00

Microporous polymeric composites from bicontinuous microemulsion polymerization using a polymerizable nonionic surfactant

L. M. Gan*, J. Liu, L. P. Poon and C. H. Chew
Department of Chemistry, National University of Singapore, Singapore

and L. H. Gan
Division of Chemistry, NIE, Nanyang Technology University, Singapore
(Received 8 January 1997)

The formation of microstructural polymeric composites by the polymerization of methyl methacrylate (MMA), 2-hydroxyethyl methacrylate (HEMA), a nonionic macromonomer ω-methoxy poly(ethylene oxide)$_{40}$ undecyl-α-methacrylate (PEO-R-MA-40) in the bicontinuous microemulsions has been successfully achieved. By photoinitiated polymerization at about 35°C, these microemulsions gelled within 30 min and transparent polymeric composites were formed on further polymerization. Various concentrations of KCNS solution were also used in the microemulsions for monitoring the variation of conductivity during polymerization. Bicontinuous structures of microporous composites were produced when the aqueous solutions in precursor microemulsions contained about 25–60 wt%. The pore sizes of these polymeric composites were generally smaller than 100 nm in diameter and they exhibited two distinctive glass transition temperatures (T_g). The higher one was about 70°C which was almost unaffected by the KCNS concentration in precursor microemulsions. This higher T_g might derive from the backbone of the copolymers. The lower T_g increased markedly from −52 to −1.8°C as the KCNS concentration increased from 0.05 to 2.5 M. It is attributed to the increasingly restricted motion of long pendant groups (side chains) of hydrophilic PEO-R-MA-40 by forming complexes with KCNS. © 1997 Elsevier Science Ltd.

(Keywords: bicontinuous microemulsion; polymerization; nonionic macromonomer)

INTRODUCTION

Microemulsions are thermodynamically stable and transparent oil–water systems stabilized by interfacial layers of surface-active agents. The interest in microemulsion lies in its ability to solubilize simultaneously larger amounts of oil and water. There are three types of microemulsions, namely oil-in-water microemulsion (o/w), water-in-oil (w/o) and bicontinuous microemulsion. The former two types of microemulsions possess droplet-like microstructures, while the latter consists of bicontinuous microstructures. The numerous number of the microstructures in each type of the microemulsion can be used as micro-reactors for polymerization to obtain ultrafine latex particles or bicontinuous polymeric materials.

The interest of the study on the formation of porous polymeric materials[1–6] by polymerizing styrene or MMA in bicontinuous microemulsions is increasing. These microemulsions were normally stabilized by non-polymerizable surfactants, such as sodium dodecyl sulfate or *n*-alkyl trimethylammonium bromide. Only recently, transparent microporous polymeric materials have been successfully prepared from microemulsion polymerization of MMA in conjunction with a polymerizable surfactant. The polymerizable surfactant used was either a cationic acryloyloxyundecyltrimethylammonium bromide[7] (AUTMAB) or zwitterionic acryloyloxyundecyldimethylammonium acetate[8] (AUDMAA).

This paper reports the formation of microstructured materials by using a nonionic polymerizable surfactant, ω-methoxy poly(ethylene oxide)$_{40}$ undecyl-α-methacrylate[9,10] (PEO-R-MA-40) in microemulsions containing MMA and HEMA. It is to explore the feasibility of using these polymerizable microemulsions to form transparent polymeric composites with the controllable pore sizes of nanometre range.

EXPERIMENTAL

Materials

MMA from BDH, HEMA and ethylene glycol dimethacrylate (EDGMA) from Merck were purified under reduced pressure to remove inhibitor before use. The photoinitiator 2,2-dimethoxy-2-phenylacetophenone (DMPA) of 99% purity was obtained from Aldrich and potassium thiocyanate (99.9%) from Baker Inc. Water was distilled twice before use. The polymerizable nonionic surfactant of ω-methoxy poly(ethylene oxide)$_{40}$ undecyl-α-methacrylate (PEO-R-MA-40) was synthesized as reported[9] recently.

Microemulsion systems

The microemulsion region was determined visually by titrating a certain amount of MMA, HEMA, and

*To whom correspondence should be addressed

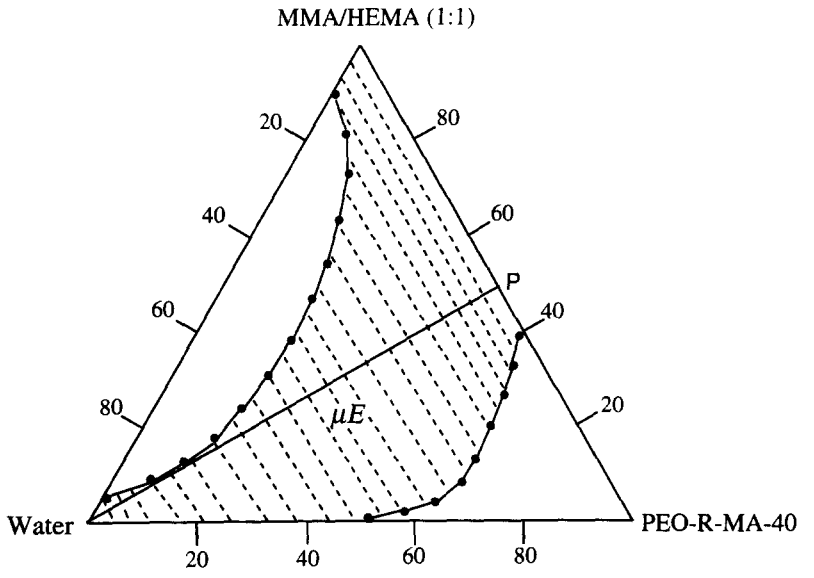

Figure 1 The partial phase diagram of MMA/HEMA/PEO-R-MA-40/water. The single-phase microemulsion region at 30°C is represented by the shaded area

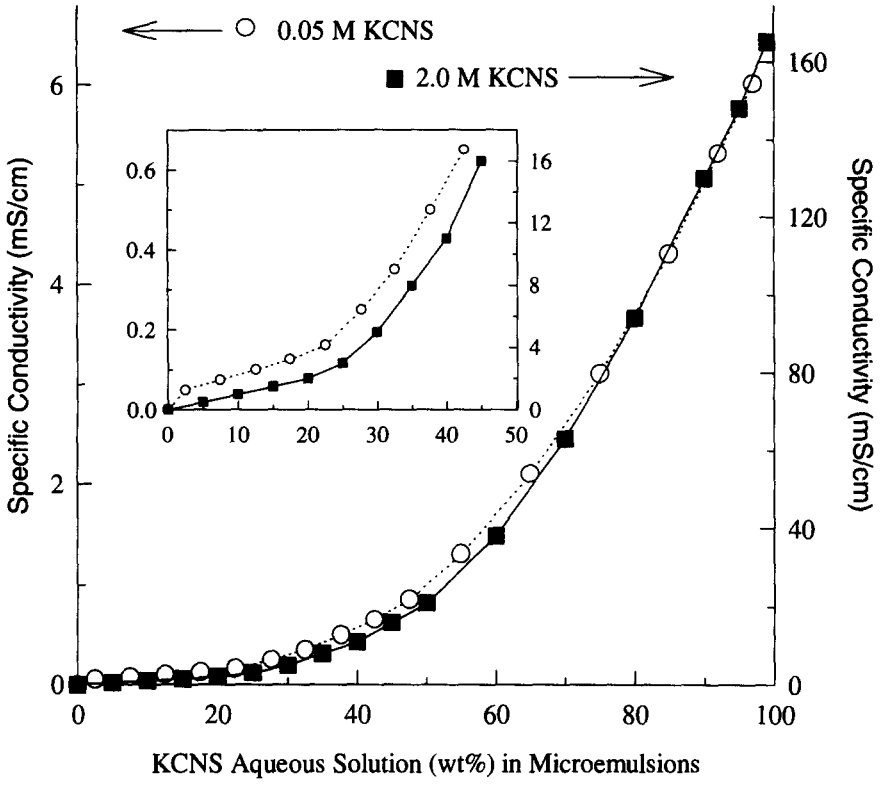

Figure 2 The variation of conductivity of the system MMA/HEMA/PEO-R-MA-40 (1/1/2) as a function of the aqueous content of 0.05 or 2.0 M KCNS solution with different concentrations

PEO-R-MA-40 with water in a screw-capped tube at room temperature (30°C). Each titration was thoroughly mixed using a Vortex mixer. The clear-turbid boundaries were established from the systematic titrations. The resulting partial microemulsion phase diagram was thus obtained as shown in *Figure 1*. From the information of conductivity measurements as shown in *Figure 2*, the type of microemulsion can thus be deduced. A MeterLab™ CDM210 conductivity meter with a cell constant of 0.78 cm^{-1} was used for the measurements.

Conductivity measurements during polymerization

The amount of microemulsion used was about 2 g to sufficiently cover the carbon electrodes. The compositions of the microemulsion samples are listed in *Table 1*. For instance, sample W20K05 (2.0 g) consisted of 20 wt% MMA (0.4 g), 20 wt% HEMA (0.4 g), 40 wt% PEO-R-MA-40 (0.8 g) and 20 wt% of 0.05 M KCNS solution (0.4 g). An additional 4 wt% EGDMA based on the total weight of both monomers was then added to each sample as a cross-linking agent. The components of each sample were well mixed in a screw-capped tube to

Table 1 Effect of the KCNS aqueous solution on the conductivity of microemulsions before and after polymerization

Sample notation	KCNS (M)	Compositions of microemulsion (wt%)[a]				Specific conductivity[b]		
		KCNS solution	MMA	HEMA	PEO-R-MA-40	κ_i (mS cm^{-1})	κ_f (mS cm^{-1})	κ_f/κ_i
W15K05	0.05	15	21.25	21.25	42.5	0.11	0.007	0.06
W20K05	0.05	20	20	20	40	0.14	0.021	0.15
W40K05	0.05	40	15	15	30	0.58	0.267	0.46
W60K05	0.05	60	10	10	20	1.65	1.32	0.80
W15K5	0.5	15	21.25	21.25	42.5	0.6	0.06	0.10
W20K5	0.5	20	20	20	40	1.0	0.17	0.17
W30K5	0.5	30	17.5	17.5	35	3.5	0.98	0.28
W40K5	0.5	40	15	15	30	4.4	2.16	0.49
W50K5	0.5	50	12.5	12.5	25	7.2	5.04	0.70
W60K5	0.5	60	10	10	20	12.1	9.80	0.81
W20K20	2	20	20	20	40	3.9	0.55	0.14
W30K20	2	30	17.5	17.5	35	6.1	1.65	0.27
W40K20	2	40	15	15	30	14.8	6.96	0.47
W50K20	2	50	12.5	12.5	25	30.4	21.89	0.72
W60K20	2	60	10	10	20	56.0	48.16	0.86

[a] Cross-linker EGDMA added was 4 wt% on the basis of the total weight of monomers used in each system, and DMPA was 0.3 wt% on the basis of the total weight of monomers

[b] The specific conductivity of the system before polymerization is denoted by κ_i and that after polymerization by κ_f

form a transparent microemulsion before it was transferred to the reaction tube by means of a syringe. Two carbon electrodes were placed in the reaction glass tube sealed with a rubber septum. After purging with nitrogen gas, the tube was then placed in a Rayonet photochemical reactor chamber for a duration of 3 h at about 35°C. The change of the conductivity was continuously monitored using a PW 9526 digital conductivity meter (Philips) during the polymerization. The polymerized microemulsion sample usually solidified in less than 30 min. The final conductivity was recorded after the polymerized sample had been left for 24 h at 30°C.

Thermal analysis

Drying rate of water desorption. The drying rate of water desorption from the polymerized samples was monitored using a Dupont Instruments TGA 2960 thermogravimetric analyser. A known size of the polymer sample was dried in a stream of dry nitrogen gas at 70°C for 3 h. It was then increased to 100°C at a ramp rate of 20°C min^{-1} and the drying was continued for 1 h in order to obtain the final weight of the polymer which was free from any moisture. The weight loss was recorded as a function of time throughout the experiment and the dimensions of samples were measured again after drying. The drying rate for the sample, based on the average of the initial and final surface area, was plotted against the free moisture content of the sample in the form of the drying-rate curve[11,12].

Glass transition temperature (T_g). The T_g of a polymer was measured using a Dupont DSC2920 Differential Scanning Calorimeter with a heating rate of 10°C min^{-1}. The initial onset of the slope of the d.s.c. curve was taken as T_g.

Thermoporometry. A Dupont Instrument DSC2920 Differential Scanning Calorimeter along with Dupont Thermal Analyst 2210 System and a Liquid Nitrogen Cooling Accessory (LCNA) were used to measure and analyse the endothermic heat effect of the polymer samples in relation to the melting of ice in the pores of the samples. About 10–20 mg of the polymerized sample was hermetically sealed in a high-pressure sample pan. The sample was placed in dry ice for 24 h to ensure complete freezing. The sample was further cooled to −40°C before a temperature ramp of 0.5°C min^{-1} was applied until 10°C. This low rate of heating was used to avoid kinetic effects. A pore volume distribution curve was obtained by analysing the d.s.c. thermogram in accordance with the thermoporometry method described by Brun *et al.*[13].

According to Brun *et al.*, the amount of undercooling ΔT for water with $0 > \Delta T > -40$ is related to the radius r of the pores by

$$r = \frac{-32.33}{\Delta T} + 0.68 \quad (1)$$

and the apparent energy of melting (W_a) which is also a function of undercooling ΔT is given by

$$W_a = -0.155\Delta T^2 - 11.39\Delta T - 332 \quad (2)$$

The pore volume distribution dV/dr evaluated from the d.s.c. thermogram obtained during the melting of ice in the pores is given by[14]:

$$\frac{dV}{dr} = \frac{\Delta T}{32.33\rho W_a} \frac{q}{d\Delta T/dt} \quad (3)$$

where ρ is the density of KCNS aqueous solutions[15], W_a the apparent energy of melting and q, measured by d.s.c., is the heat flux required for the melting.

Equilibrium swelling

The polymer sample was cut into discs having a thickness of about 1 mm and then dried to a constant

weight in a vacuum oven at room temperature. They were swelled in water at 30°C. Periodically the discs were removed from water, blotted lightly to remove excess surface water and weighed. The equilibrium water content (EWC) expressed as percentage is given by

$$\mathrm{EWC}(\%) = \frac{W_s - W}{W_s} \times 100 \qquad (4)$$

where W_s and W refer to the weights of the swollen polymer sample at equilibrium swelling and the dried polymer sample respectively.

Leaching of polymer solids

The final cross-linked polymer samples were dried under vacuum to constant weights. The dried samples were then immersed in water and put in an oven at a constant temperature of 50°C for six days. Water was replaced once a day with fresh distilled water. The weight loss was attributed to KCNS, the unreacted monomers and macromonomer, and possibly the homopolymer of PEO-R-MA-40, which is water soluble.

RESULTS AND DISCUSSION

Characterization of microemulsion system

The system composes water, MMA, HEMA, PEO-R-MA-40 and a small amount of crosslinker EGDMA. Besides being a comonomer, HEMA also acts as a cosurfactant for the system. In the absence of HEMA, there are two separate isotropic regions. However, when HEMA was added to the ternary system, a large single isotropic region was formed as shown in *Figure 1*. The enlarging single phase region, by the effect of cosurfactant HEMA, is attributed to the increased flexibility of the curved oil–water interfaces of the system. Thus the alignment of the orderly arranged micellar aggregates in the liquid crystalline region becomes less favourable and it shifts to the isotropic microemulsion region.

A conductivity measurement has been commonly used in identifying the microstructural type of an ionic microemulsion. It is known that w/o and o/w microemulsions will show very low and very high conductivity respectively. Moreover, the transition from a w/o to a bicontinuous microemulsion exhibits a sharp increase in conductivity. Since the components of microemulsions of H_2O/MMA/HEMA/PEO-R-MA-40 are not conductive, various concentrations of KCNS salt were added to the microemulsions which could then be characterized by conductivity measurements along line P in *Figure 1*. The variation of conductivities of microemulsions with aqueous solutions of 0.05 M and 2.00 M KCNS is presented in *Figure 2*. Both salt concentrations in the same microemulsion showed a similar trend of a low conductivity at lower aqueous solutions (<25%), followed by a sharp increase in conductivity when the aqueous solution was greater than 25% as can be clearly seen from the inset of *Figure 2*. The conductivity of the microemulsion continued to increase exponentially with the increase of the aqueous solutions up to about 70 wt%. Beyond which, the conductivity of the microemulsion increased linearly. The low conductivities for the systems with the aqueous solutions less than 25 wt% were due to the formation of w/o microemulsions with aqueous droplets dispersed in the oil medium. The

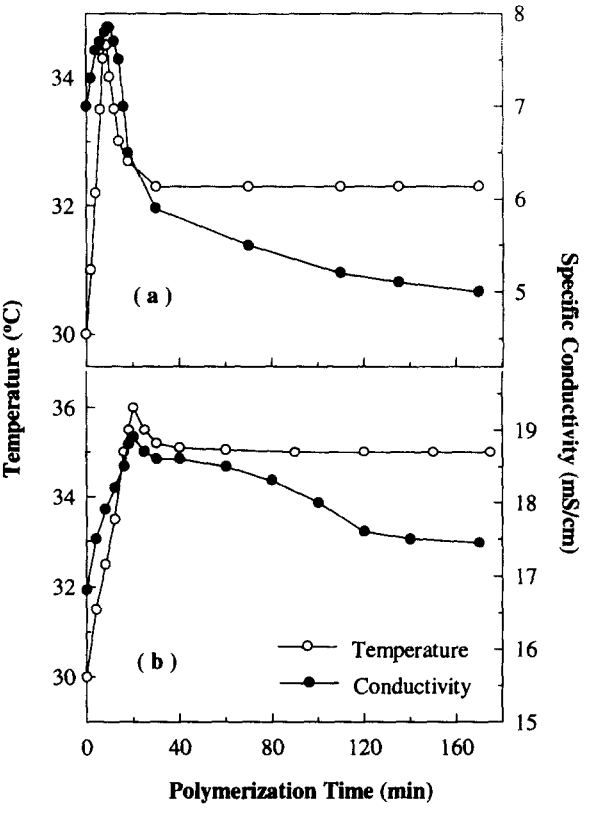

Figure 3 The changes of conductivity and temperature during the polymerization for samples (a) W40K5 and (b) W60K5

increase of the aqueous solutions (>25%) in the system resulted in the formation of bicontinuous microemulsions. This is evidenced by the sharp increase in conductivity due to the presence of numerous interconnected conducting channels. It is envisaged that the systems with the aqueous solutions ranging from about 25–70% were in the form of bicontinuous microemulsions. However, no distinction can be made between the bicontinuous and oil-in-water microemulsions at an aqueous solution higher than 70 wt% by this conductivity measurement.

Change of conductivity in polymerization of microemulsions

The conductivities of precursor microemulsions containing different amounts of 0.5 M KCNS aqueous solution were monitoerd up to the completion of polymerization. The variations of conductivity and temperature during polymerization for samples W40K5 and W60K5, with compositions shown in *Table 1*, are depicted in *Figure 3*. Both samples showed sharp increases in conductivity and temperature to their maxima within 30 min of polymerization. They then decreased and approached constant values. Many other microemulsion systems with different amounts of KCNS concentrations also exhibited the similar behaviour during polymerization.

The initial sharp increase in the conductivity is attributed to the increase of sample temperature. This is because the temperature in the photoreactor was higher (33°C) than that (29°C) of the unreacted sample. As the polymerization started, heat also gave off causing the sample temperature to exceed (>33°C) the temperature of the reactor. The peak temperature of a sample was attained when the polymerization was at its

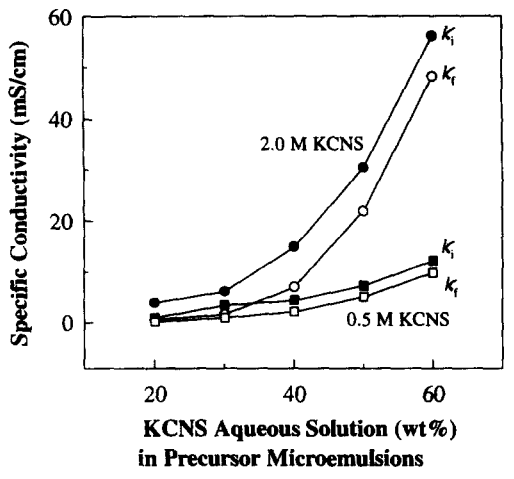

Figure 4 The variation of conductivity of microemulsions before polymerization (κ_i) and after polymerization (κ_f) as a function of KCNS aqueous contents in precursor microemulsions

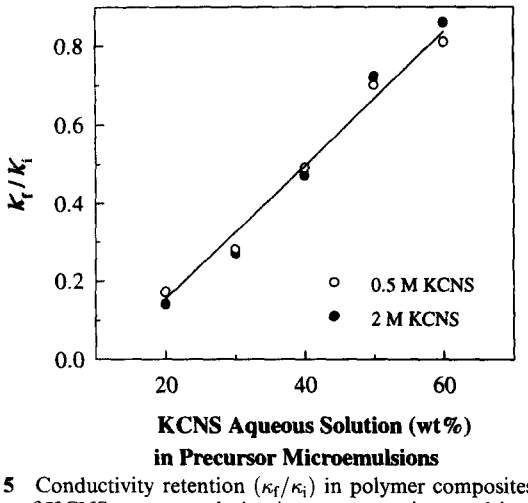

Figure 5 Conductivity retention (κ_f/κ_i) in polymer composites as a function of KCNS aqueous solution in precursor microemulsions

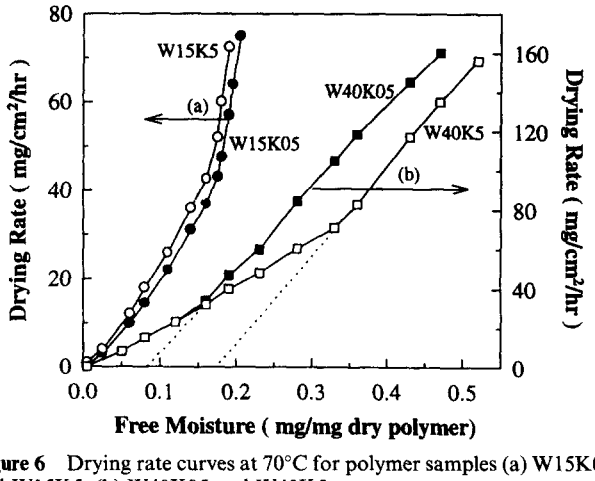

Figure 6 Drying rate curves at 70°C for polymer samples (a) W15K05 and W15K5, (b) W40K05 and W40K5

maximum rate. When the polymerization proceeded with a slower rate, the sample temperature also decreased until it equilibrated with the temperature of the reactor. The variation of conductivity was in parallel with the temperature change in the early state of polymerization. Once a polymerized microemulsion was transformed to a transparent solid polymer, its conductivity was further reduced arising from the phase change of the system. In addition, the conductive aqueous channels of the microstructures might also have been modified or became narrower during the process of polymerization. This explains the continuous slight decrease of conductivity as even the sample temperature had reached an equilibrium.

Figure 4 shows the increase of specific conductivity of microemulsions before (κ_i) and after polymerization (κ_f) as a function of KCNS aqueous solution in precursor microemulsions. The detailed compositions of these microemulsions can be found from *Table 1*. When the ratio of κ_f/κ_i is plotted against the amount of KCNS solution in microemulsions, a linear relationship is obtained for two KCNS concentrations as shown in *Figure 5*. The value of κ_f/κ_i may be interpreted as the extent of conductivity retention by a polymerized microemulsion. The higher the value of κ_f/κ_i, the lesser modification would be on the microstructures of precursor microemulsion after polymerization. If we assume the conductivity of a bicontinuous microemulsion is proportional to the average area (πr^2) of its conducting aqueous channels, i.e. $\kappa_f \propto \pi r_f^2$ and $\kappa_i \propto \pi r_i^2$, then $r_f/r_i \propto (\kappa_f/\kappa_i)^{1/2}$. Hence, a value of 0.81 for κ_f/κ_i is proportional to a value of 0.9 for r_f/r_i. This may imply that there is about 10% reduction in the average radius of the conducting aqueous channels arising from the polymerization of a fluid microemulsion to a transparent solid polymer. This simple argument is based on the assumption that there is no blockage of conducting channels during polymerization. If a slight blockage of channels did occur, the actual reduction of the average radius of the conducting channels would be even smaller than 10%.

Thermal analysis on polymerized microemulsions

After polymerization, a solid polymer in cylindrical shape (shape of the reaction tube) was obtained. The diameter and height of the samples were about 1.2 cm and 1.8 cm respectively. They were transparent and mechanically stable polymer solids. They could be fractured or ground to powder after they were frozen in liquid nitrogen. Since all the polymerized microemulsions were crosslinked by EGDMA, their physical dimensions remained unchanged after drying. Thus the pore volumes of the dried samples were approximated to the volume of the aqueous solutions occupied in the precursor microemulsions. They might range from about 0.2 to 0.6 $cm^3 g^{-1}$ of dried samples. The bulk density of the dried materials thus varied from about 0.4–0.8 $g cm^{-3}$ dependent on the aqueous solution content in each precursor microemulsion.

Drying rate of water desorption. Additional information pertaining to the continuity of the pore structures of polymerized microemulsions in the solid form can be derived from the thermogravimetric analysis. The exponential decay in the falling rate period for the polymeric composites W15K05 and W15K5 shown in *Figure 6* is a characteristic of closed-cell type microstructures. These composites were transformed from the precursor microemulsions containing only 15 wt% KCNS aqueous solution of two concentrations, i.e. 0.05 or 0.5 M. On the other hand, composites obtained from precursor microemulsions containing ≥20 wt% KCNS aqueous solution show the linear falling-rate period followed by

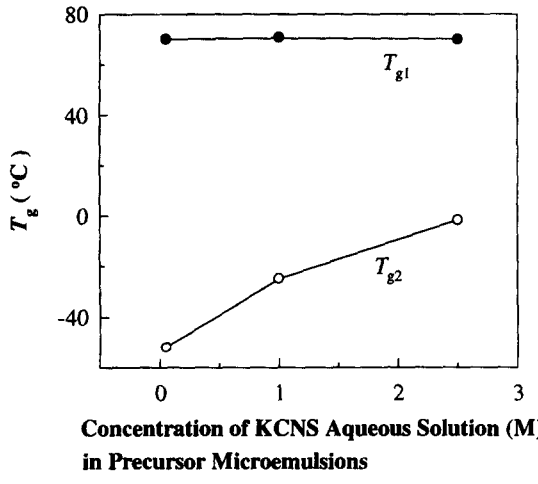

Figure 7 Glass transition temperatures of vacuum-dried polymeric solids from precursor microemulsions containing 40 wt% KCNS aqueous solution of various concentrations

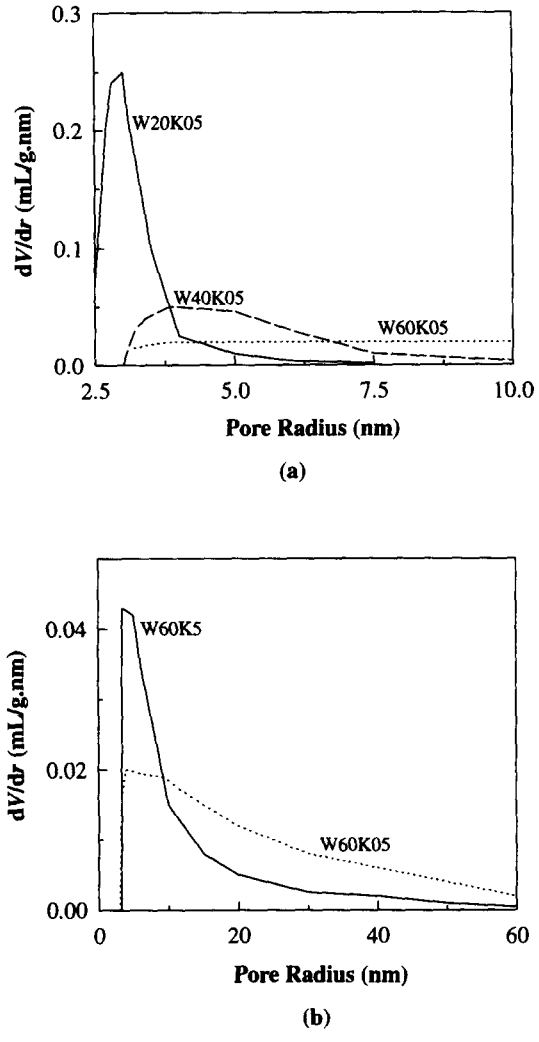

Figure 8 Pore volume distributions for polymer samples (a) W20K05, W40K05 and W60K05, (b) W60K05 and W60K5

an exponential decay[11,16]. This drying rate behaviour is typical of open cell porous solids such as samples W40K05 and W40K5, as shown in *Figure 6*. These polymeric composites contained 40 wt% aqueous solution of either 0.05 or 0.5 M KCNS. However, their drying rate curves did not superimpose on each other. This may be due to the formation of different amounts of KCNS crystals in the internal channels of the open-cell structures during the latter stage of drying. The salt crystals might have then blocked the water channels and prevented the remaining water to flow freely to the surface. Under such a circumstance, the open-cell structure of the polymeric composite would have been changed to the closed-cell type structure and its drying rate of water desorption would decrease exponentially. With a higher KCNS concentration (0.5 M) in the composite W40K5, an expected early onset of exponentially decaying in drying rate is thus observed in *Figure 6*.

Glass transition temperature (T_g). The polymerized microemulsions in the form of polymer composites exhibit two distinctive glass transition temperatures. For instance, *Figure 7* shows the T_gs for the vacuum-dried polymeric composites prepared from precursor microemulsion containing 40 wt% aqueous solution of various KCNS concentrations. The T_{g1} of about 70°C was almost unaffected by the change of KCNS concentration. But T_{g2} increased from −52, −25 to −1.8°C as the KCNS concentration was increased from 0.05, 1.0 to 2.5 M respectively. The T_g of pure PEO-R-MA-40 is −64.9°C.

The observed two sets of T_gs for the polymerized microemulsions are believed to be derived from the hydrophobic backbone of the copolymer (T_{g1}) and its long pendant group of hydrophilic PEO (T_{g2}). This is because all these precursor microemulsions contained three reactive monomers, namely MMA, HEMA and PEO-R-MA-40 with the chemical structure of $CH_2{=}C(CH_3)COO(CH_2)_{11}(OCH_2CH_2)_{40}OCH_3$. Since these monomers possessed the same polymerizable group of $CH_2{=}C(CH_3)COO^-$, they would form copolymers with the same backbone structure having different small side chains and a long pendant group of $-(CH_2)_{11}(OCH_2CH_2)_{40}OCH_3$. Since T_{g1} is believed to be associated with the hydrophobic backbone of the copolymers, the effect of KCNS concentration on T_{g1} will be insignificant as observed. On the other hand, the pendant hydrophilic PEO group of PEO-R-MA-40 would have been solubilized in the aqueous domains (channels) of precursor microemulsions and remained there even after polymerization to form polymer composites. Under this circumstance, the pendant PEO could form complexes with KCNS as has been reported[17]. Thus T_{g2} increased with the KCNS concentration due to the increasing reduction in PEO segmental motion in the form of KCNS complexes.

Thermoporometry. The pore volume distribution curves for polymer composites W20K05, W40K05, W60K05 and W60K5 are shown in *Figure 8*. The pore size distributions were in the range of about 2–4 nm for sample W20K05, 3–12 nm for W40K05, 3–100 nm for W60K05 and 3–60 nm for W60K5. The results indicate an increase in the pore sizes of the polymerized microemulsions with increasing aqueous content of the precursor microemulsions. The similar trend has also been observed for other systems[18]. In addition, the concentration of KCNS also affected the pore volume distribution as shown in *Figure 8b*. It indicates that sample W60K5 with a higher KCNS concentration (0.5 M) had a much narrower pore size distribution than that of W60K05 (0.05 M KCNS). The majority of pore sizes for the

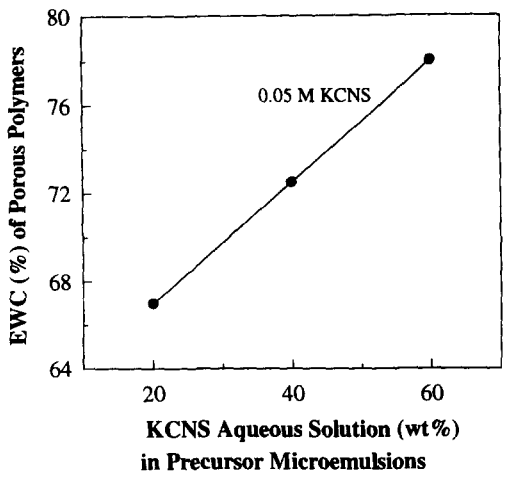

Figure 9 Equilibrium water content (EWC) for polymers as a function of 0.05 KCNS aqueous solution in precursor microemulsions with compositions shown in *Table 1*

former ranges from about 3–20 nm in radius. This is likely due to the narrowing effect by a higher KCNS deposition on the inner walls of water channels during the thermoporometric measurements.

Swelling characteristics of porous polymers

The equilibrium water contents (EWC) for porous polymeric composites W20K05, W40K05 and W60K05 are shown in *Figure 9*. The EWC of the composites increased linearly with the increased amount of 0.05 M KCNS aqueous solution in their precursor microemulsions. This is expected because the porosity of the bicontinuous structural polymers would increase with increasing aqueous content in precursor bicontinuous microemulsions as has been observed in the polymerized zwitterionic AUDMAA microemulsion system[19]. These porous polymeric composites also had low leached contents in hot water after being dried in vacuum. For examples, sample W20K05, W40K05 and W60K05 lost only 0.43, 0.98 and 1.67 wt% respectively. The weight loss may be due to KCNS and possibly traces of unreacted monomers and macromonomer. Hence, it is believed that the reactive monomers of MMA, HEMA, and PEO-R-MA-40 in these microemulsions were well copolymerized and crosslinked via EGDMA.

CONCLUSIONS

A new type of transparent microporous polymeric composites has been prepared by microemulsion polymerization of MMA, HEMA, and a polymerizable nonionic surfactant of PEO-R-MA-40. The pore dimension (<100 nm) of these microstructural composites can be varied by simply adjusting the aqueous content in precursor microemulsions. Bicontinuous polymeric composites will be formed when the aqueous contents in precursor microemulsions are in the range of about 25–60 wt%. These polymeric composites can readily be crosslinked by EGDMA to enhance their mechanical strengths. This novel polymerizable microemulsion system can also be used for making ultrafiltration membranes. This is the subject of our next paper.

ACKNOWLEDGEMENT

The authors are grateful to the National University of Singapore for financial support under grant RP950605 and RP950606.

REFERENCES

1. Sasthav, M. and Cheung, H. M., *Langmuir*, 1991, **7**, 1378.
2. Palani Raj, W. R., Sasthav, M. and Cheung, H. M., *Langmuir*, 1992, **8**, 1931.
3. Gan, L. M., Chieng, T. H., Chew, C. H. and Ng, S. C., *Langmuir*, 1994, **10**, 4022.
4. Chieng, T. H., Gan, L. M., Chew, C. H. and Ng, S. C., *Polymer*, 1995, **36**, 1941.
5. Chieng, T. H., Gan, L. M., Chew, C. H., Ng, S. C. and Pey, K. L., *J. Appl. Polym. Sci.*, 1996, **60**, 1561.
6. Chieng, T. H., Gan, L. M., Chew, C. H., Ng, S. C. and Pey, K. L., *Polymer*, 1996, **37**, 2801.
7. Li, T. D., Chew, C. H., Ng, S. C., Gan, L. M. and Teo, W. K., *J. Macromol. Sci., Pure Appl. Chem.*, 1995, **A32**, 969.
8. Gan, L. M., Li, T. D., Chew, C. H. and Teo, W. K., *Langmuir*, 1995, **11**, 3316.
9. Liu, J., Chew, C. H. and Gan, L. M., *J. Macromol. Sci., Pure Appl. Chem.*, 1996, **A33**, 337.
10. Liu, J., Chew, C. H., Wang, S. Y. and Gan, L. M., *J. Macromol. Sci., Pure Appl. Chem.*, 1996, **A33**, 1181.
11. McCabe, W. L., Smith, J. C. and Harriot, P., in *Unit Operations of Chemical Engineering*, 4th edn. McGraw-Hill, New York, 1985, p. 716.
12. Palani Raj, W. R., Sasthav, M. and Cheung, H. M., *J. Appl. Polym. Sci.*, 1993, **47**, 499.
13. Brun, M., Lallemand, A., Quinson, J. F. and Eyrand, C., *Thermochim. Acta*, 1977, **21**, 59.
14. Nakao, S., *J. Membrane Sci.*, 1994, **96**, 131.
15. Lobo, V. M. M., in *Handbook of Electrolyte Solutions*, Part A. Elsevier, New York, 1989, p. 1104.
16. Coulson, J. M. and Richardson, J. F., in *Chemical Engineering*, Vol. II, 2nd edn. Pergamon, New York, 1968, p. 620.
17. Xie, H. Q., Liu, J. and Xie, D., *Eur. Polym. J.*, 1989, **25**, 1119.
18. Sasthav, M., Palani Raj, W. R. and Cheung, H. M., *J. Colloid Interface Sci.*, 1992, **152**, 376.
19. Chew, C. H., Gan, L. M., Ong, L. H., Zhang, K., Li, T. D. and MacDonald, P. M., Submitted to *Langmuir*.